

Gum 48d: an evolved HII region with ongoing star formation

J.L. Karr

Academia Sinica Institute of Astronomy and Astrophysics, Taipei, Taiwan, ROC

P. Manoj

Department of Physics and Astronomy, University of Rochester, NY

N. Ohashi

Academia Sinica Institute of Astronomy and Astrophysics, Taipei, Taiwan, ROC

ABSTRACT

High mass star formation and the evolution of HII regions have a substantial impact on the morphology and star formation history of molecular clouds. The HII region Gum 48d, located in the Centaurus Arm at a distance of 3.5 kpc, is an old, well evolved HII region whose ionizing stars have moved off the main sequence. As such, it represents a phase in the evolution of HII regions that is less well studied than the earlier, more energetic, main sequence phase. In this paper we use multi-wavelength archive data from a variety of sources to perform a detailed study of this interesting region. Morphologically, Gum 48d displays a ring-like faint HII region associated with diffuse emission from the associated PDR, and is formed from part of a large, massive molecular cloud complex. There is extensive ongoing star formation in the region, at scales ranging from low to high mass, which is consistent with triggered star formation scenarios. We investigate the dynamical history and evolution of this region, and conclude that the original HII region was once larger and more energetic than the faint region currently seen. The proposed history of this molecular cloud complex is one of multiple, linked generations of star formation, over a period of 10 Myr. Gum 48d differs significantly in morphology and star formation that the other HII regions in the molecular cloud; these differences are likely the result of the advanced age of the region, and its different evolutionary status.

Subject headings: star formation;HII Regions;triggered Star formation; HII regions: individual(Gum 48d,RCW 80)

1. Introduction

High mass star formation has a profound impact on the interstellar medium, through a combination of effects including ionizing radiation and expanding HII regions, stellar winds and supernovae. The effects and appearance of high mass star formation vary dramatically throughout the evolution of an OB star. When a high mass star begins burning hydrogen, it produces significant amounts of UV radiation, which immediately start to ionize the surrounding neutral and molecular gas. At very early stages, the star is still heavily embedded in its natal cloud, surrounded by a small (0.1 pc) ultra-compact HII region (UCHII), and visible only at radio and infrared wavelengths. The region then expands into a classic HII region. At this phase of evolution, the OB star(s) are surrounded by a hot bubble of ionized gas, the Stromgren Sphere, initially a few parsecs in size, which due to the pressure imbalance expands into the ambient medium and compresses the surrounding molecular material.

The HII region, now several parsecs or more in size, is bright in both radio (free-free and recombination line emission) and optical (particularly $H\alpha$ emission). The heating of dust grains in the vicinity of the region leads to bright emission from dust in the mid to far-infrared, particularly in the photodissociation region (PDR) between the ionized and molecular gas. If the star forming region contains multiple OB stars, the HII region can evolve into a giant HII region as individual HII regions combine to form an extended, often irregularly shaped ionized region up to 100 pc in diameter. Ongoing star formation is generally seen surrounding the HII region.

During the main sequence and later post-main sequence phase the ionizing stars can experience significant mass loss in the form of super-sonic stellar winds. These winds expand into the already ionized HII region, creating a stellar wind bubble, and eventually deposit their mechanical energy into the surrounding ISM (Arthur 2007). In the final stages, supernova explosions from the OB stars can expand into the combined HII region/stellar wind bubble, further disrupting the remnants of the original molecular cloud (Garcia-Segura and Franco 1996).

At the very end of the HII region evolutionary sequence only the remnants of the violent disruptions of the molecular cloud remain; shells and super shells of neutral material that have been swept up through the combined effects of the HII region, stellar winds and supernova remnants, eventually slowing down and fragmenting (Tenorio-Tagle and Bodenheimer 1988). By this point, the presence of the initial high mass ionizing stars is inferred from the shape of the ISM, as the ionizing stars have long since progressed through the main sequence to the later stages of evolution, to supernovae, to the point where even the SNR are no longer readily observable.

The detailed effects of high mass star formation on the ISM and on subsequent star formation activity are complex and contradictory. The expanding HII region, stellar winds and supernovae will eventually combine to disrupt the natal molecular cloud. At shorter timescales there is a significant influx of energy into the cloud, increasing turbulence as well as potentially truncating circumstellar disks. On the other hand, HII regions have long been thought to enhance star formation in molecular clouds through triggered or sequential star formation (Elmegreen 1998). The expanding HII region can compress existing overdensities in the molecular material, leading to instability and collapse; the RDI or radiatively driven implosion model (Lefloch and Lazareff 1994). Alternatively, a shell of material can be swept up around the expanding ionized region, eventually becoming unstable, fragmenting and collapsing into new stars; the collect and collapse model (Elmegreen and Lada 1977). Quantifying the effects of an HII region on the star formation rate of a region (or even attempting to ‘prove’ a proposed example of triggered star formation), is non-trivial, and in the case of an individual HII region often inconclusive.

The classic HII region, ionized by one or more stars, is to date the best studied of the various stages of evolution of the HII region, due to its high brightness, relatively large size and the fraction of the lifetime of an HII region spent in this phase. The UC/CHII phase is relatively short (a few 10^5 years) compared to the classic/giant HII region phase, which is on the order of the main sequence lifetime of the ionizing stars: approximately $1-7 \times 10^6$ years depending on the initial masses of the stars.

The shorter lived post main sequence phase involves a change in the effective spectral type of the star and a corresponding drop in the total flux of ionizing photons compared to the main sequence, resulting in an extended but fainter HII region in the radio and optical. The later phases, including the SN phase, are transitory. The final remnant shell phase is longer lived but observationally elusive, due to the absence of strong ionizing radiation and the complexity of the interstellar medium in neutral hydrogen, making the positive identification of remnant shells difficult.

The HII region Gum 48d, located in the Centaurus Arm, presents an interesting example of the post main sequence phase of a classic HII region. The region is ionized by a B0I_p supergiant, HR 5171B, with a companion G8 Ia supergiant, HR 5171A, a high luminosity, extremely variable star (a.k.a. V766 Cen, HD 119796), of interest in its own right (Humphreys et al. 1971; van Genderen 1992). The region was initially identified in the Gum and RCW catalogs of optical HII regions as Gum 48d and RCW 80 respectively (Gum 1955; Rodgers et al. 1960). Some subsequent studies identify it as RCW 80 (Georgelin et al. 1988; Humphreys et al. 1971; Saito et al. 2001), while others confuse it with a radio bright supernova remnant to the south (Whiteoak and Green 1996; Rakowski et al. 2001; Green 2004).

The distance to the SNR region has been variously estimated as 4 kpc, 5.4 kpc and 7.8 kpc (Guseinov et al. 2004), and is most likely at a further distance than the HII region. For clarity we will keep the identification Gum 48d for the HII region and RCW 80 for the SNR.

In this paper we use multi-wavelength archived survey data from various sources to investigate Gum 48d. Multi-wavelength archive data provide a powerful tool for the study of extended HII regions. The use of multiple wavelengths allows us to probe the different components of the ISM; from hot ionized gas to cold molecular gas to dust, as well as tracing the population of embedded stars. Archived data, on the other hand, permits the exploration of large regions of sky, and the discovery and selection of interesting HII regions which would not necessarily be readily selected for more specific, pointed observations.

In Section 2 we outline the sources and utility of the archive data used. In Section 3 we discuss the multi-wavelength morphology, ionization and structure of the region. In Section 4 the star formation content at various mass scales is investigated. We then discuss the dynamic evolution and history of the region, including its local history (Section 5.1) and speculate as to the possibility of triggered star formation caused by Gum 48d (Section 5.2). Finally, the position of Gum 48d in the larger scale structure and evolution of the region is discussed in Section 5.3.

2. Data

There are a number of archived data sets available for this region. The region was observed as part of the Spitzer GLIMPSE Legacy Survey of the inner galaxy, at 3.6, 4.8, 5.6 and 8 microns, all with a resolution of about $1'.2$ (Benjamin et al. 2003). All the bands except 4.8 microns contain emission features from Polycyclic Aromatic Hydrocarbons (PAHs), large, complex interstellar molecules. PAHs absorb UV radiation and re-emit in various mid-infrared spectral features. The 8 micron band, in particular, contains two of the strongest PAH features, at 7.7 and 8.6 μm . Emission from PAHs is an excellent tracer of photodissociation regions (PDRs), the interface between neutral and molecular hydrogen, as PAHs are destroyed by shock fronts in the interior of ionized regions, and are effectively shielded from UV radiation in dense molecular material. The 4.8 micron band contains a rotational line of shocked molecular hydrogen, while all four bands also contain thermal emission from small grains.

In addition to the GLIMPSE data we have used archive data from the MIPS-GAL survey at 24 microns, a longer wavelength companion survey to GLIMPSE. At this wavelength, the relevant emitter is small dust grains, which may or may not correspond to the PAH

morphology, depending on the physical conditions in the region; PAH emission and warm dust continuum generally coincide, but warm dust frequently exists in the absence of PAH emission.

Point source catalogs are available for both the GLIMPSE data and the 2 Micron All Sky Survey (2MASS), the later at J, H and K_s (Skrutskie et al. 2006). We have performed point source extraction on the 24 micron data archive data (which are of good quality) and combined the results with the preceding two catalogs to create 1-24 micron spectral energy distributions (SEDs) for all point sources in the region. The point source SEDs provide an excellent tracer for young stellar objects (YSOs), due to the strong near and mid-infrared emission from protostellar disks and envelopes, and the low extinction at these wavelengths.

Optical images were obtained from the Southern H Alpha Sky Survey Atlas (SHASSA) (Gaustad et al. 2001), with a resolution of 1'. Radio continuum (1420 MHz) and line (HI 21 cm) data sets at 1' were obtained from the Southern Galactic Plane Survey (SGPS) (McClure-Griffiths et al. 2005). Both data sets trace the morphology and brightness of the ionized gas, through H α and free-free emission respectively. The optical data are strongly affected by extinction, unlike the radio data, and so the combination can provide a probe of three dimensional HII region morphology.

3. Gum 48d

Figure 1 shows the large scale structure of the region surrounding Gum 48d on a two degree scale; 1420 MHz emission, tracing ionized gas in HII regions and SNRs, is shown in blue, GLIMPSE 8 micron data, tracing PAH emission PDRs, is shown in green, and 24 micron MIPS GAL data, tracing warm dust, is shown in red. The contours show the location of molecular gas (¹³CO(J=1-0)) in the velocity range of the Centaurus Arm, from the survey of Saito et al. (2001). Individual HII regions in the area are labeled, while the region containing Gum 48d is outlined with a box.

The emission from ionized gas is shown in Figure 2, in optical (left panel) and radio (right panel). The optical emission in H α shows a faint, semi-circular nebulosity surrounding the central star. The central star seen in the image is HR 5171A, the high luminosity G8 Ia supergiant which dominates the optical and mid infrared images. It is a binary star, whose companion, HR 5171B, is a much fainter B0 Ip supergiant and source of ionization for the region. The two stars have a kinematic distance of 3.9 kpc and a photometric distance of 3.5 kpc (Humphreys et al. 1971). If we place the two stars on an HR diagram evolutionary track, using the models of Schaller et al. (1992), HR 5171A has an age of 3.5

Myr and a main sequence mass of $60 M_{\odot}$, while HR 5171B has an age of 4 Myr and a main sequence mass of $40 M_{\odot}$, corresponding to main sequence spectral types of O7 and O5.5 respectively (Schaerer and de Koter 1997). This is consistent with the conclusions of van Genderen (1992). This implies that Gum 48d was once a very energetic HII region, ionized by multiple massive O stars. The above studies of this region identify only two stars in this system. An inspection of the Tycho catalog shows two stars at the location of HR 5171B with similar optical magnitudes, which might indicate the possibility of an additional star. No spectral information is available to confirm this, but the ionization balance calculations shown in Section 5.1 rule out the need for an additional ionizing source. We will discuss the evolutionary history of Gum 48d in more detail in Section 5.1.

The optical morphology is mirrored in the radio data. The radio image is dominated by the SNR RCW 80 to the south-west of Gum 48d. The ionized gas of the HII region has measured velocities of -48 km s^{-1} (Georgelin et al. 1988), corresponding to a near kinematic distance of 4 kpc, using the galactic rotation model of Brand and Blitz (1993). This value is in good agreement with the distances to the central stars. There are five other 1420 MHz features in the region of Figure 2. Gal 309.54-0.737 is an HII region with a velocity of -43 km s^{-1} (Caswell et al. 1981). The other four are compact 1420 MHz sources without known velocities. G309.14-0.18 is a small but extended HII region with a spectral index consistent with an HII region (Caswell et al. 1992), while G309.17-0.02, G309.27-0.03 and G309.24-0.18 have no spectral index measurements. All four sources are positionally coincident with extended emission at 24 and/or 8 microns, as described in the following section.

3.1. Dust and Gas

In the mid-infrared Gum 48d has a striking morphology, as seen in Figure 3. The main feature is an extended, bow shaped region of reasonable thickness compared to its full extent, and centered on a bright infrared point source (HR 5171A). The morphology within the region is complex and detailed on smaller scales, with significant substructure. There is a small, bright region to the very south-east of the image, corresponding to the HII region Gal 309.54-0.737, as well as a number of bright, compact mid-IR features scattered along the bow shaped region. There are also small, arc-shaped structures, most noticeably one to the east of the center of the image. Finally, there are several infrared dark clouds, seen in extinction (areas of no emission) in the 8 micron map, silhouetted against brighter emission, and a large number of infrared point sources.

This morphology is mirrored at 24 microns, as seen in Figure 4. In this image, tracing the location of warm dust, the substructure and compact features are even more prominent

than at eight microns. The locations of the compact features (discussed more fully in Sections 4.1 and 4.2) are marked in Figure 4. Several of the infrared dark clouds persist at 24 microns, while others are now seen in emission. There are two saturated regions in the 24 micron image, one corresponding to HR 5171B (the central region) and one to the AGB star GLMP 363, to the south west. Post main sequence stars are often extremely bright in the mid-infrared, due to the presence of surrounding dust.

Saito et al. (2001) conducted $^{13}\text{CO}(J=1-0)$ observations of this region, identifying an extensive molecular cloud at velocities corresponding to the Centaurus Arm of the galaxy and a kinematic distance of 3.2 - 5.5 kpc, with a total mass of $2.3 \times 10^6 M_{\odot}$; an extremely massive molecular complex. The whole molecular cloud observed by Saito et al. (2001) is shown in Figure 1. The molecular cloud forms an extensive “ridge” perpendicular to the Galactic plane and with a physical extent of 80 pc. This molecular ridge curves slightly, and Gum 48d is located at its inner edge.

Saito et al. (2001) also carried out $\text{C}^{18}\text{O}(J=1-0)$ observations in the same region to investigate more detailed structures of the molecular cloud, identifying several dense molecular cores. The locations of the C^{18}O molecular cores are marked in Figure 3; diamonds mark the location of cores with velocities corresponding to Gum 48d, crosses mark cores at more negative velocities. The C^{18}O is arrayed around the edge of the 8 micron PAH emission, outside of the emission from the ionized gas, with velocities ranging from -40.6 to -50.2 km s^{-1} . This demonstrates that the bulk of the 8 micron emission occurs at the interface between the ionized region and the molecular cloud. In addition, it can readily be seen that the locations of the infrared dark clouds are coincident with the positions of the C^{18}O dense cores. These infrared dark clouds are very dense, often filamentary clouds of molecular material that are optically thick in the mid-infrared (Carey et al. 1998), and are sometimes associated with highly embedded, very young protostars. We note that the smaller arclike 8 micron feature located at $309.4 - 0.37$ is associated with molecular gas at -60 km s^{-1} . This region is either not physically associated with Gum 48d, or it is located at the front of the HII region cavity, and is moving towards us with respect to the central velocity of the ionized gas.

The HII region Gal 309.54-0.737 is associated with a molecular cloud at -52.6 km s^{-1} . Its morphology at 24 and 8 microns, when compared with the 1420 MHz emission and location of the molecular cloud, is indicative of a compact blister HII region, sharply bounded to the south east and venting to the north-west. The region shows a strong alignment between the location of the emission of ionized gas and mid-infrared emission from dust. The nebula is only very faintly seen in the optical, at the unbounded north-west edge, corresponding to the fainter radio emission of the venting gas.

The other four compact HII features are all associated with features at 24 and 8 microns.

G309.14-0.18 is associated with an infrared dark cloud at 8 microns, but with clumpy emission at 24 microns, brighter to the western edge (denoted S10 in Figure 4). G309.17-0.02 is associated with compact emission at both 24 and 8 microns (denoted S11 in Figure 4), while G309.27-0.03 is associated with compact emission at only 24 microns (denoted S12 in Figure 4). G309.24-0.18 is located near an arc like structure at 8 microns and faint interior emission at 24 microns (denoted S4 in Figure 4). The molecular emission components are not well aligned, however, and most likely are the result of a coincidental projection onto G309.24-0.18.

The velocities of the molecular material are consistent with the published values for the ionized material, and have kinematic distances consistent with the photometric distance of the ionizing star. That, combined with the morphological correspondence between the dust, molecular and ionized emission, indicates that all observed components of the region are located at a distance of 3.5 kpc and are physically associated with each other.

4. Star Formation

Gum 48d shows extensive, ongoing star formation over a range of masses. Low and intermediate mass star formation is well traced in the near to mid-infrared, with several methods of identifying young stars based on infrared photometry available. The first is by color; at IRAC wavelengths young stars show redder colors, with more embedded sources being progressively more red (Allen et al. 2004). At these wavelengths, extinction is minimal and shows little variations with wavelength (Indebetouw et al. 2005). A complementary technique is the measurement of the mid-infrared spectral slope, α , using the definitions of Adams et al. (1988). Sources with rising mid-IR slopes are identified as Class I sources, young stars still heavily embedded in their molecular envelope. Those with negative slopes that are shallower than photospheric emission are Class II sources (Classical T-Tauri and Herbig Ae/Be stars), which are less embedded but still have a significant circumstellar disk, and possibly remnant envelope. An additional category, flat-spectrum sources, straddles the boundary between the two. The even younger Class 0 sources, are not well identified by this method, due to the extreme extinction at shorter wavelengths.

There are a total of 48411 2MASS sources, 39176 GLIMPSE catalog sources and 517 extracted MIPS 24 micron sources in the region shown in Figure 3. The three catalogs were combined to produce a single band merged catalog; this final catalog contains 76696 sources. Of these, 12670 have sufficient fluxes for an IRAC color-color diagram (i.e. fluxes are measured in all four IRAC bands). The IRAC color-color diagram is shown in Figure 5. The sources at 0,0 are photospheric SEDs, with more embedded (redder) sources occurring

to the upper right.

We also calculate the mid-infrared spectral slopes for all sources with photometry in at least four bands between 2MASS K_s and IRAC 8 microns (21284 sources), and identify Class I, Flat Spectrum and Class II sources, for a total of 1827 sources. The classification based on the mid-infrared SED slope is, in general, very well correlated with the classification via IRAC colors, however the method is more robust in the presence of a missing IRAC flux. Figure 6 shows the distribution of young stars identified above over the region. In the upper panel Class I sources are marked with crosses and flat spectrum sources with diamonds, shown over the IRAC 8 micron image and tracing the most embedded phase of star formation. In the lower panel the location of Class II sources are shown with triangles.

There are several sources of contamination in method for identifying potential YSOs; foreground and background galactic and extragalactic sources. The high levels of extended emission in the mid-infrared minimizes the contamination by faint background sources, either galactic or extragalactic, as the detection limits at 24 and 8 microns are generally limited by background levels rather than sensitivity to the point source flux. Unresolved star forming galaxies have IRAC colors indistinguishable from young stars; however, the location of this region in the Galactic plane, combined with the low flux of many of these sources, minimizes this contamination. For comparison, we took a nearby region in the sky, of similar galactic latitude, without an HII region in either the optical or radio, and without bright features in the mid-infrared, and determined the number of sources with YSO colors. This gives us an estimate of the line of sight contamination of sources. The region from $l=309.56$ to 310 and $b=-0.273$ to -0.705 was the largest potential region; if we scale the YSO counts to match the angular size of the Figure 6 the expected contributions from line of sight contaminants are 2%, 14%, and 29% for Class I, Flat Spectrum and Class II sources respectively.

At the distance of Gum 48d the 2MASS fluxes are of limited usefulness, due to the typical limiting magnitude of the survey. Only the brightest and/or reddest of the young stars at 3.5 kpc will be detected, due to both the intrinsic luminosity and the high extinction in the Galactic plane. The IRAC and MIPS data are considerably more sensitive to objects with the SEDs of YSOs and are much less affected by extinction. K_s band fluxes are the most commonly detected, and are useful for the calculation of the spectral slope in cases where one of the IRAC fluxes is missing.

In this region the Class II sources are primarily correlated with the large molecular ridge, indicating ongoing star formation throughout the cloud, even though Class II sources have a higher level of contamination through background or foreground sources. The more heavily embedded Class I and flat spectrum sources, however, are more strongly clustered. There are several clusters or small aggregates of very embedded young stars, many of which

are associated with dense cores identified in $\text{C}^{18}\text{O}(J=1-0)$. The locations of the clusters, determined by eye, are marked in the first panel of Figure 6. A cluster at 309.42-0.64 is associated with a clump with a central velocity -42.4 km s^{-1} , one at 309.53-0.75 with central velocity of -52.6 km s^{-1} , one at 309.22-0.47 with a clump with a central velocity of -40.6 km s^{-1} , and at 309.14-0.19 with material at -46.4 km s^{-1} . A cluster at 309.38-0.14 is associated both with a molecular clump with a velocity of -50.5 km s^{-1} and with a maser (a star formation tracer) at -50 km s^{-1} (Caswell et al. 1995). All of these velocities are consistent with the velocities of the HII region and its constituent components. A final cluster at 309.54-0.12 is not associated with a high density region, although it is superposed on extended ^{13}CO emission. From this distribution it is apparent that star formation is continuing throughout the molecular ridge, and that the most embedded phases of star formation are preferentially occurring in the densest molecular gas; many of these clusters are also associated with IR dark clouds.

Age estimates of young stars are difficult to derive, as stars of different masses evolve at different rates, and even stars of similar masses can show a range of different spectral slopes for a given age, due in part to the effects of orientation (Robitaille et al. 2007). The general consensus, however, is that rising and flat spectrum sources are, on average, a younger and more embedded phase of star formation (Allen et al. 2004). Thus, the younger population of young stars is more highly clustered than the older population.

4.1. Intermediate Mass Star Formation

In addition to the IRAC point sources tracing primarily low and intermediate mass star formation, there is evidence for ongoing star formation at higher masses. There are a number of infrared features throughout this region, which share the common properties of being bright, compact (less than a few arcseconds) and clearly non-point sources while at the same time not being diffuse. Some of the sources are associated with emission from ionized gas, while others are not. We will divide the sample into two groups; intermediate and high mass star formation, based on the absence or presence of emission from ionized gas. Intermediate mass star formation is discussed below, while high mass star formation is discussed in Section 4.2.

The first sample of infrared sources shows compact but distinctly non-point like morphology at 24 microns, and compact but structured morphology at 8 microns. Figure 7 shows a gallery of these sources, while Table 1 lists the positions, angular sizes, physical sizes (assuming a distance of 3.5 kpc) and 8 and 24 micron fluxes. The 24 micron flux is in general smoothly distributed, even considering the larger 24 micron PSF, but occupies

the same physical extent as the more structured 8 micron emission. To confirm this, we convolved the 8 micron data with the 24 micron PSF for comparison. These sources do not show an obvious 24 or 8 micron embedded point source, and show no evidence of compact or point like 1420 MHz emission at the sensitivity of the SGPS survey. The diameters of the sources range from 0.5 - 2 pc.

A possible explanation for these sources is that they are enshrouded intermediate mass stars (Fuente et al. 1998, 2002; Roger and Dewdney 1992; Diaz-Miller et al. 1998). The lack of radio continuum emission associated with these sources argues against the presence of an UCHII region and therefore rules out the presence of stars earlier than type B1, as a UCHII region around more massive stars at this distance would be visible at the sensitivity of the radio data. On the other hand, bright, extended 8 micron emission is often indicative of a photodissociation region, which can be created by sub-Lyman ultraviolet radiation. The 24 micron emission traces warm, small grained dust, which can also be heated by sub-Lyman photons. Intermediate mass stars of type later than B1 could satisfy these irradiation conditions, while stars lower in mass than B8 would not provide enough ultraviolet radiation to illuminate a strong PDR. The lack of a clearly defined point source within the region could be due to sensitivity, extinction, or the high level of mid-IR emission making point sources difficult to detangle from the structured, extended emission, a particular problem at 24 microns.

Although there are no distinguishable point sources within the compact features, there is a spatial correlation between the compact features and the embedded young stars, which strengthens the claim that they are associated with ongoing star formation. Sources S7 and S8 are associated with a small aggregate of deeply embedded sources, as well as a maser source, while S3 is at the edge of another small aggregate. Sources S5 and S6 are associated with the star formation at the inner edge of the HII region, and S1 and S2 are associated with another concentration of embedded star formation. Source S9 is located near the heavily embedded star formation of Gal 309.54-0.737, as well as a small cluster of highly embedded sources. These positional coincidences indicate that these sources are physically related to star formation in this region; they are unlikely to be foreground or background projections.

Kerton (2002) identified 165 potential candidates similar to those described above based on CO data in the Canadian Galactic Plane Survey and MSX 8 micron survey data, with a limiting distance of 2 kpc, indicating that these might not be particularly rare objects. The objects shown here are of comparable size (1-2 pc in diameter) to the objects in the MSX sample, albeit of smaller angular size. We computed IRAS luminosities and colors for those sources with IRAS counterparts (S1, S2, S3, S7, S8, S10 and S11), as tabulated in Table 1. The luminosities, sizes and colors are all within the range found by Kerton (2002).

We attempted to duplicate the HI velocity analysis performed therein, but did not have sufficient spatial resolution in the 21 cm data to reach a conclusion. The SGPS data are of similar resolution to the previous study, but the sources are more distant by a factor of at least two than those sources.

It should be noted that at a distance of 3.5 kpc a B0 star would be expected to have a visual magnitude of at least 14.7, and a B5 star 18.0, using the standard value of 1.6 magnitude of extinction per kpc in the Galactic plane. The actual magnitude of an enshrouded B star could be much greater due to the high density cocoon of material. Therefore, we are unlikely to detect an enshrouded B star at this distance in the available survey data. High sensitivity NIR observations could provide a probe of the embedded B star and potential lower mass cluster.

Sources S7 and S8 show a particularly interesting morphology; a vaguely bi-polar structure (two lobed) with several deeply embedded sources (24 micron bright) in between. The morphology is reminiscent of a bi-polar outflow with a wide opening angle. The SEDs and 8 and 24 micron morphologies are similar of those of the other compact sources which have been identified as possible enshrouded B stars. This might be an outflow near an enshrouded star, or could possible be a pair of enshrouded B stars in a cluster of young stars. The lack of bright IRAC Band 2 data (tracing molecular shocks) argues against the first option, as do the SEDs. Therefore, these are most likely to be enshrouded B stars.

It is worth considering the likelihood of observing an intermediate mass B star in this phase, as these are not widely observed objects. Estimates of the ages of this class of objects vary, however, consensus is that they are less than 10^6 years old (Fuente et al. 1998, 2002; Roger and Dewdney 1992; Diaz-Miller et al. 1998). The general lack of associated masers indicates a relatively evolved status (Kerton 2002). This is a longer timescale than the typical estimated ages of UCHII regions (up to a few 10^5 years), a much better studied class of object. A young, enshrouded B star would not be identified through radio surveys, the typical method of discovery for UCHII regions, and mid-IR data suitable for a general search have only recently become generally available. Furthermore, an enshrouded B star would only be detected with this morphology under the right conditions. In a lower density environment the B star could more easily break out of its cocoon, while in the close presence of ionizing stars the observational signature of the B star would be overwhelmed. Therefore, the relative lack of previous studies of these objects is likely the result of both the difficulty of detecting them in previously available data and the combination of factors required to make them detectable in the infrared.

4.2. High Mass Star Formation

There is further evidence for ongoing high mass star formation in this region, as traced by emission from ionized gas. The infrared morphologies of the high mass star formation candidates are shown in Figure 8 (S9, S10, S11 and S12; see also Table 1), while the HII regions themselves are labeled in Figure 2, with additional information in Table 1. In general, the high mass star formation candidates show more extended emission in the infrared than the intermediate mass candidates. The first source, S10, is associated with the HII region, G309.14-0.18 which coincides with an IR-dark cloud at 8 microns, a bright arc along the west side and bright, clumpy emission (including several bright point sources) at 24 microns. The IR-dark cloud is associated with one of the C¹⁸O clumps observed by Saito et al. (2001), with a velocity of -46.4 km s⁻¹ and with a cluster of embedded young stars, as discussed above. The 1420 MHz radio emission has a spectral index consistent with an HII region and is resolved in the 1' resolution SGPS data. The ionizing star is not known and is undetectable at optical or mid-IR wavelengths due to the high foreground extinction.

To the south of Gum 48d there is another high mass star formation region, Gal 309.54-0.737, a blister HII region. This HII region is clearly identified as an HII region by its spectral index, although the ionizing star is not seen due to high extinction. The velocity of the C¹⁸O emission associated with this region (-52.6 km s⁻¹) corresponds to the Centaurus Arm, although Saito et al. (2001) place it at the far kinematic distance, based on the lack of associated optical emission. However, the region is actually visible in the H α data in the northwest (corresponding with the direction of the champagne flow), although it is extremely faint. Therefore it is likely that the faintness of the region in the optical is due to strong local extinction, rather than the region being at a significantly larger distance than the other HII regions in the area.

Though the ionizing stars associated with these two compact HII regions are unknown, we can use the 1420 MHz flux to estimate the spectral type of the star required to produce the ionizing flux necessary to maintain the observed free-free emission, using the radio free-free spectral luminosity

$$\frac{N_{Ly}}{s^{-1}} \approx 6.3 \times 10^{52} \left(\frac{T_e}{10^4 K}\right)^{-0.45} \left(\frac{\nu}{GHz}\right)^{0.1} \left(\frac{L_\nu}{10^{20} W Hz^{-1}}\right)^{-1} \quad (1)$$

where N_{Ly} is the flux of ionizing photons, T_e is the electron temperature and L_ν is the observed luminosity at frequency ν . This calculation has several uncertainties. It assumes ionization equilibrium. The calculated value will be a lower limit, as a matter bounded HII region will leak ionizing flux into the surrounding lower density medium. In addition, the ionizing flux could be the result of multiple, lower mass stars rather than a single, higher mass

star. Gal 309.54-0.737 has a background subtracted flux of 1.6 Jy at 1420 MHz, a distance of 3.5 kpc and an electron temperature of 5900 K (Caswell and Haynes 1987). These values give a Lyman flux of 1.5×10^{47} , corresponding to a main sequence spectral type of B0.5 (Vacca et al. 1996). The calculated Lyman flux of G309.14-0.08 is below the model values for OB stars, indicative of its young age. This implies that these HII regions are ionized by single stars, unless significant ionizing flux is escaping from these regions. This is unlikely due to the extremely dense surrounding material.

There are two further HII regions with mid-infrared counterparts. The compact HII regions G309.17-0.02 is associated with a compact feature at 8 and 24 microns (S11) and is morphologically similar to the B star candidates, but its spectral index and velocity are not known. The region at G309.27-0.03 is associated with compact emission at 24 microns only (S12), although there is a faint arc like 8 micron feature at its edge.

To summarize the star forming properties of this region:

- There is extensive, ongoing, low mass star formation associated with the molecular material surrounding Gum 48d.
- The more embedded and younger phases of star formation are more strongly clustered than the more evolved Class II sources, and are strongly correlated with the densest molecular material.
- There is evidence for intermediate mass star formation, in the form of potential enshrouded B1-B8 stars. These sources are also correlated with the location of molecular material and low mass star formation.
- There are five UC-small HII regions in the area, indicating high mass star formation. Four of them are positively identified with either a cluster of embedded young stars, or molecular material at Centaurus arm velocities, indicating a physical association with Gum 48d.

5. Discussion

In the following discussion, we attempt to describe the dynamical and star formation history of Gum 48d, and its place in the large scale structure and history of the Centaurus arm region. In Section 5.1 we describe the dynamical history of Gum 48d, using known physical parameters, and compare it with values predicted by models for the expansion of an HII region. In Section 5.2 the proposed history and the current observed star formation

activity are compared to evaluate the region in the context of triggered star formation. Finally, in Section 5.3 Gum 48d is compared with other HII regions in the area, and its place in the large scale structure and star formation history of the Centaurus arm is analyzed.

5.1. History of Gum 48d

In this subsection, we attempt to describe the history of Gum 48d, illustrated in panels (a) to (d) in Fig. 9. We then discuss Gum 48d’s atypical appearance when compared to other nearby HII regions in the context of this history.

As briefly discussed in Section 3, Gum 48d is currently ionized by HR 5171B, a B0 I_p post-main sequence star. This is fully consistent with a spectral type estimation of the ionizing star using Equation 1 and the 1420 MHz radio flux of Gum 48d. We should note, however, that the duration of the post-main sequence phase is short compared to the main sequence lifetime of the ionizing stars, suggesting that the dynamical evolution of Gum 48d and its expansion into the surrounding ambient material will have been mostly determined when HR 5171 B and its companion, HR 5171A, were in the main sequence phase, with spectral type of O5.5 and O7, respectively (see Section 3).

How much did Gum 48d extend into the surrounding ambient material when the two ionizing stars were in the main sequence phase? The expansion of an HII region into a uniform density ambient medium can be simply described by the model of Dyson and Williams (1997), in which

$$\frac{R}{\text{pc}} \approx 4.5 \left(\frac{N_{\text{Ly}}}{10^{49} \text{s}^{-1}} \right)^{1/7} \left(\frac{n}{10^3 \text{cm}^{-3}} \right)^{-2/7} \left(\frac{t}{\text{Myr}} \right)^{4/7} \quad (2)$$

R is the radius of the HII region, N is the flux of ionizing photons, n is the ambient density of the surrounding material, and t is the time scale of the expansion, which should be equivalent to the age of the ionizing star. Based on the main sequence masses and spectral types of HR 5171A and B, estimated using an HR diagram in Section 3, the time scale of the expansion and the ionizing flux during the main sequence phase are 3.8 Myr and 1.1×10^{50} photons s^{-1} , respectively. If we assume that the radius of Gum 48d during its main sequence phase is the same as its current size, 8.4 pc measured from the radio free-free emission at 1420 MHz, the estimated ambient density of the original molecular cloud is $5.7 \times 10^3 \text{cm}^{-3}$, an unreasonably high value for a molecular cloud. For comparison, the average density of the current molecular ridge is 500cm^{-3} , estimated from its averaged column density, $1.9 \times 10^{22} \text{cm}^{-2}$ (Saito et al. 2001), assuming that the molecular ridge is of a similar physical scale

along the line of sight as it is in width.

There are several possible explanations for the discrepancy between the calculated value for the density and physically plausible values. One scenario is blow-out; if the HII region breaks out of the ambient material into a lower density region, a champagne flow will occur. This will slow the expansion of the HII region into the denser medium (Tenorio-Tagle 1979). Another possibility is that the HII region created during its main sequence phase was larger than the currently ionized region. This makes more sense physically because the difference between the ionizing fluxes during the main sequence and post main sequence phases is substantial, and we would expect a more energetic HII region in the past. For example, the W5-West HII region, with an ionizing flux half that of Gum 48d during its main sequence phase, has a current radius of 35 pc (Karr and Martin 2003). Similarly, the wind blown bubble models of Arthur (2007) for a 40 solar mass star predict a final radius at the end of the stellar wind phase of on order of 30 pc.

How do we recognize the maximum size of Gum 48d during the main sequence phase? One potential way is to use the PAH emission at 8 microns arising from the PDR region, which occurs at the interface between the molecular and neutral gas, and can be excited by sub-Lyman UV photons. Consequently, it is a better tracer of the edge of the molecular shell than the emission from ionized gas. The material surrounding the HII region forms a roughly semi-circular shell, illuminated by the PAH emission. The molecular ridge is significantly larger in scale than the PAH shell around Gum 48d, as is indicated in panel (d) of Figure 9.

The recombination timescale for ionized hydrogen is approximately $10^5/n$ years, where n is the number density of the gas. The timescale for the formation of molecular hydrogen from atomic hydrogen is approximately $10^9/n$ (Tielens and Hollenbach 1985). For a typical HII region density of 10 cm^{-3} this corresponds to 10,000 and 10^8 years respectively. Therefore, in the time since HR 5171B has left the main sequence and the ionizing flux has dropped, there has been sufficient time for the ionized region to recombine into atomic hydrogen, but not to re-form molecular hydrogen, leaving an extended neutral envelope around the current HII region.

If we take this PAH shell as the boundary of the original HII region, the radius of the HII region is roughly estimated to be 15 pc when measured across the carved out semi-shell. The ambient density calculated via the model above is now 840 cm^{-3} , approaching physically plausible values. It should be noted that the HII region is not spherically symmetric, and the radius estimated changes somewhat with the assumed geometry of the HII region. The assumed shape and center of the PAH shell were chosen as an intermediate estimate of the size of the partial shell.

The current structure and appearance of Gum 48d therefore seem to be the result of its evolutionary status. The shape of the surrounding molecular/neutral material is dominated by the large scale structure of the molecular ridge and the actions of the energetic main sequence phase, while the current ionization state is the product of the post main sequence star, HR 5171B. Gum 48d differs significantly in appearance when compared with nearby, more typical HII regions, where the ionized region borders directly on a bright PDR (as discussed further in Section 5.3). Unlike these regions, the PDR and the edge of the ionized regions are not congruent in Gum 48d, and the PDR is fainter and more diffuse.

5.2. Triggered Star Formation

When studying HII regions and ongoing star formation, the question of triggered star formation inevitably arises. Is the ongoing star formation a consequence of the effects of the expanding HII region on the surrounding ISM? Proving this conclusively is problematic at best. Typical methods involve 'not disproving' the hypothesis, often by assembling a consistent time line for the different phases of star formation.

The best case for triggered star formation in this region, given its age and morphology, is the collect and collapse model, where the expanding HII region compresses the surrounding material and sweeps up a shell of dense gas. At some point, the dense shell becomes unstable, fragments, and collapses to form stars (Elmegreen and Lada 1977). In order for a region to be consistent with a triggered star formation scenario, the time from the formation of the ionizing star and turning on of the associated HII region to the gravitational instability and fragmentation of the swept up shell, plus the age of the putatively triggered star formation population must be comparable to the total age of the region.

As discussed earlier, the age of Gum 48d is $\simeq 4$ Myr, based on the ages of the ionizing stars. The age of the YSO population is not easily calculated, and it is not possible to perform such a calculation from the mid-infrared SEDs alone. However, a typical age for embedded low mass YSOs is on the order of or less than 1 Myr. It is difficult to assign a precise age for the embedded B star phase of intermediate mass star formation, but their lifespan is estimated at < 1 Myr years (Dewdney et al. 1991; Roger and Dewdney 1992). The age of UCHII regions are also not well understood, largely due to uncertainties in modeling the early stage of expansion, but they are a similarly young phase of star formation (a few times 10^5 years (Garcia-Segura and Franco 1996)). To summarize, the ages of the various populations of young stars at different masses are on order of 1 Myr or less.

This leaves the epoch of the fragmentation of the shell to be determined. This can be

estimated via a simple analytical model. Following the equations of Whitworth et al. (1994), which progress from the expansion model of Dyson and Williams (1997) used earlier, a shell created around an expanding HII region becomes unstable to fragmentation and collapse at a time

$$\frac{t_{frag}}{\text{Myr}} \approx 1.56 \left(\frac{a_s}{0.2\text{km s}^{-1}}\right)^{7/11} \left(\frac{N_{Ly}}{10^{49}\text{s}^{-1}}\right)^{-1/11} \left(\frac{n}{10^3\text{cm}^{-3}}\right)^{-5/11} \quad (3)$$

a_s is the sound speed (0.2 km s⁻¹ an extreme lower limit), n is the number density of the ambient medium (10³ cm⁻³ an extreme upper limit) and N_{Ly} is the flux of ionizing photons. At this point the HII region and its corresponding shell have reached a radius

$$\frac{R_{frag}}{\text{pc}} \approx 5.8 \left(\frac{a_s}{0.2\text{km s}^{-1}}\right)^{4/11} \left(\frac{N_{Ly}}{10^{49}\text{s}^{-1}}\right)^{1/11} \left(\frac{n}{10^3\text{cm}^{-3}}\right)^{6/11} \quad (4)$$

with the variables as described above. Using the estimated size of the original HII region calculated from the molecular/PAH shell (15 pc) we can then work backwards; solving for the initial density from the current size via Equation 4, and then calculating the fragmentation timescale from Equation 3. For a sound speed $a_s = 0.5$ km s⁻¹ this gives an estimate of the fragmentation timescale of 3.1 Myr and an initial ambient density of 490 cm⁻³, comparable to the current density of the extended molecular ridge. The fragmentation timescale could be decreased if the ionizing stars were to depart from the main sequence, which corresponds to a decrease in ionizing radiation and subsequent cooling of the swept up shell.

This time scale for fragmentation, plus the ages of the various populations of young stars of different masses (about 1 Myr), is comparable in age to the original HII region. Therefore, the star formation can be explained as the result of triggering by the original HII region. The locations of the enshrouded B stars are significant in this scenario, as they are located around the larger PAH shell (corresponding to the original HII region) rather than the smaller, currently ionized region. This is also consistent with formation via triggering and the collect and collapse model.

More detailed modeling of Gum 48d would be problematic due to the non-static large scale structure. The HII region has formed and evolved in an expanding, increasingly more massive giant ridge of molecular material. This type of dynamically changing environment in the surrounding ISM and its interaction with an evolving HII region is beyond the scope of current models.

5.3. Large Scale Structure

Gum 48d is part of a large molecular complex containing a significant amount of star formation activity; this region is shown in the three color image of Figure 1. This molecular complex is one of the most massive in the galaxy ($2.3 \times 10^6 M_{\odot}$ as traced by $^{12}\text{CO}(J=1-0)$) and forms a massive ridge in CO with velocities corresponding to the Centaurus Arm (Saito et al. 2001). The CO ridge is associated with an even larger ridge in neutral hydrogen.

There are a number of HII regions associated with this ridge. All of the HII regions are associated with high mass condensations in the molecular ridge and have velocities consistent with the Centaurus Arm; their locations are marked in Figure 1. Gum48d, Gal 309.1+0.2, Gal 309.8+0.5 and Gal 309.54-0.737 are associated with the molecular supershell, while RCW 79 is located slightly to the north-west. Gal 309.54-0.737 shows the classic morphology of a young blister HII region, while Gal 309.1+0.2, Gal 309.8+0.5 and RCW 79 show prototypical main sequence HII region morphologies.

This entire region is studied in more depth in Karr et al. (2008). In that paper, the masses of the ionizing stars needed to maintain the current 1420 MHz luminosity were calculated using the free-free continuum luminosity. The Dyson and Williams (1997) model for HII region expansion was used to estimate the ages of the regions. The radio luminosities are consistent with each HII region being ionized by a single OB star (ranging from O9.5 to O6.5 for all the regions) and the expansion timescales are consistent with the HII regions being in the 1-3 Myr age range, with ionizing sources still firmly on the main sequence.

As discussed in Section 5.1, Gum 48d is significantly different from these regions in both morphology and star formation content. The emission from ionized gas is faint and diffuse in the radio, where extinction is not a factor. The morphology of the region is structured on small scales and the star-formation in the region includes compact HII regions and enshrouded B-stars in addition to low mass star formation. The other HII regions are bright in the radio, with clearly defined HII region morphologies and shell like PDR regions directly bordering on the bright HII regions. They show neither the compact features of Gum 48d nor secondary intermediate and high mass star formation indicative of triggering, although there is still significant low mass star formation. On the other hand, they, contain bright rims, cometary globules and other characteristic morphological features of the classic HII region which are absent in Gum 48d. These differences point to a significantly different evolutionary phase of Gum 48d from that of the classic HII regions.

The proposed history of the star formation over this whole region is one of multiple, linked generations of star formation, as illustrated schematically in Figure 9. The first generation of stars, forming 10 Myr ago and consisting of multiple OB stars, culminated in a series

of supernovae explosions 4-6 Myr in the past. The combined energy of the HII regions, stellar wind and supernovae created an extensive, massive expanding supershell/ridge around the region, as discussed in Saito et al. (2001). A second generation of star formation commenced in the expanding supershell some 1-3 Myr ago, producing the extended HII regions currently seen in the molecular ridge. A third generation of highly embedded star formation is seen around the individual HII regions, corresponding to star formation triggered by the HII region itself. This scenario is discussed more fully in Karr et al. (2008).

Gum 48d itself, however, does not fit cleanly into any of the three phases of star formation. In addition to the morphology and star formation differences discussed above, it is also of a significantly different age. The previous generation and progenitor of the molecular and neutral supershell/ridge is supposed to have formed around 10 Myr ago, a factor of 2.5 greater than our derived ages for the ionizing stars of the region. For the timescales estimated in Saito et al. (2001), Gum48d could be one of the first of the second generation of young stars, or possibly one of the last of the first. The latter option is the more plausible given the relative time scales.

The motion of Gum 48d's ionizing stars give further support to this scenario. The Hipparcos proper motions for HR 5171 are $-5.89 \text{ mas/year} \pm 1.38$ and $-3.66 \text{ mas/year} \pm 1.58$ for RA and Dec respectively (Perryman and ESA 1997). This results in a proper motion coming from inside the large supershell, consistent with the premise that the HR 5171 binary system was formed in the expanding supershell/ridge of material now seen as the giant molecular cloud.

The molecular material in the vicinity of Gum 48d has a higher column density than that seen in the vicinity of the other regions (as seen in Figure 1). This may be an intrinsic property of the surrounding shell, or may be the result of compression of the existing material by Gum 48d. If the former, this could explain the earlier formation of the region, as its more massive stars condensed out of the densest portions of the molecular ridge. Being more massive, the stars progressed through the main sequence more quickly, resulting in the current striking morphological differences.

Finally, there are some interesting (if purely speculative) considerations regarding the possibility of triggered star formation and the associated timescales. Gum 48d is the only region in this molecular ridge that shows significant evidence for triggered star formation on intermediate and high mass stars. It is also the oldest of the regions by 1 to 2 Myr. Is the timescale for the triggering of high mass star formation longer than that required for lower mass stars? Answering this question is beyond the scope of this paper, but a comparison with other highly evolved, late type HII regions could prove interesting.

6. Summary

- Gum48d is an old, highly evolved HII region in a post-main sequence phase that is the remnant of a larger, more energetic main sequence HII region. The current morphology of the molecular gas and PDR region reflects this history, as does the faint remnant HII region seen in the radio and optical. The region has progressed through the classic main sequence HII region phase and is now in a late HII region phase (before the existence of supernovae and a remnant molecular shell). This represents an interesting and not particularly well studied phase of HII region evolution.
- There is significant ongoing star formation associated with Gum 48d at a variety of masses. Low mass young stars are seen throughout the molecular cloud, with the more embedded, younger phases being more highly clustered and associated with the densest molecular gas. Intermediate mass star formation, in the form of enshrouded B stars, and high mass star formation, in the form of compact HII regions, are seen around the periphery of the molecular/neutral PAH shell and are similarly clustered. The timescales of expansion, fragmentation and star formation are consistent with triggered star formation by the collect and collapse model.
- Gum 48d is part of a much larger molecular cloud complex consisting of a very massive expanding partial supershell/ridge of molecular and neutral material, the result of a previous generation of massive star formation 10 Myr ago. The ridge contains a number of HII regions with ages in the 1-3 Myr range, but Gum 48d is unique in its older age, diffuse radio morphology, extended PDR and variety of secondary star formation. While the other regions are clear candidates for secondary star formation within the expanding molecular supershell/ridge, Gum 48d is most likely the first and highest mass of these triggered massive stars, and consequently in a later state of spectral evolution.

This paper makes use of data from the Southern H-Alpha Sky Survey Atlas (SHASSA), which is supported by the National Science Foundation, and The Two Micron All Sky Survey, which is a joint project of the University of Massachusetts and the Infrared Processing and Analysis Center/California Institute of Technology, funded by the National Aeronautics and Space Administration and the National Science Foundation.” The Australia Telescope is funded by the Commonwealth of Australia for operation as a National Facility managed by CSIRO.

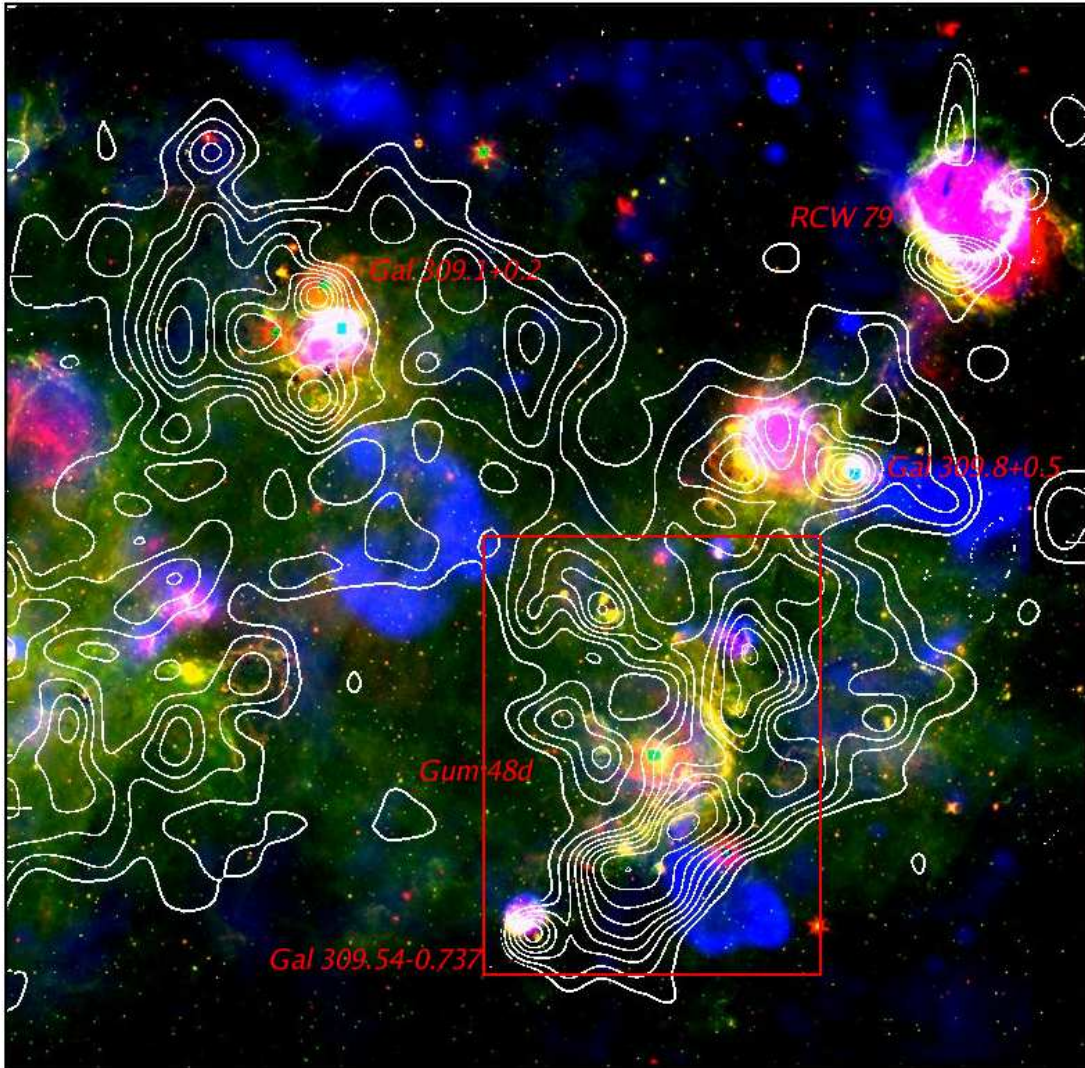


Fig. 1.— Multi-wavelength morphology of the Centaurus Arm. Blue shows 1420 MHz emission tracing ionized gas (HII regions and SNR), green shows the 8 micron GLIMPSE image tracing PAH emission (PDR Regions), and red shows the 24 micron MIPS GAL image, tracing warm dust. The contours show the location of ^{13}CO emission at Centaurus Arm velocities, from Saito et al. (2001). The HII regions at Centaurus Arm velocities are labeled, and the region of Gum48d is marked with a box.

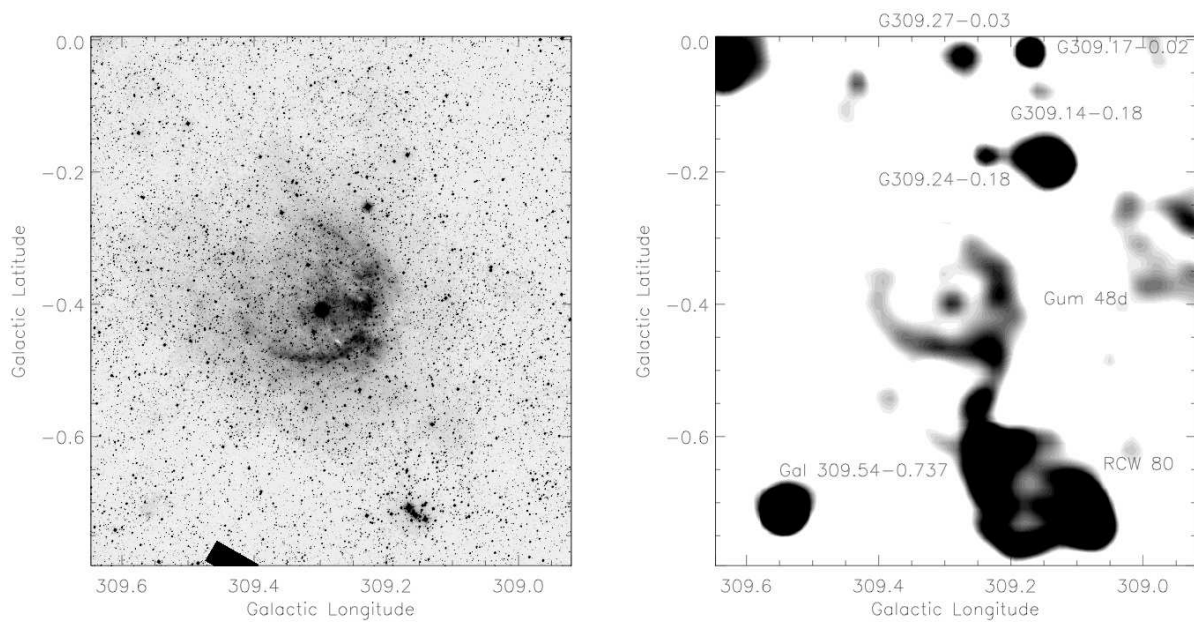


Fig. 2.— Emission from ionized gas in the vicinity of Gum 48d. The left panel shows the optical emission ($H\alpha$): Gum 48d is clearly seen as a semi-circular nebulosity. The right panel shows the lower resolution 1420 MHz radio emission from the same region. The radio emission is dominated by the SNR RCW 80, but Gum 48d is also clearly seen. HII regions are labeled.

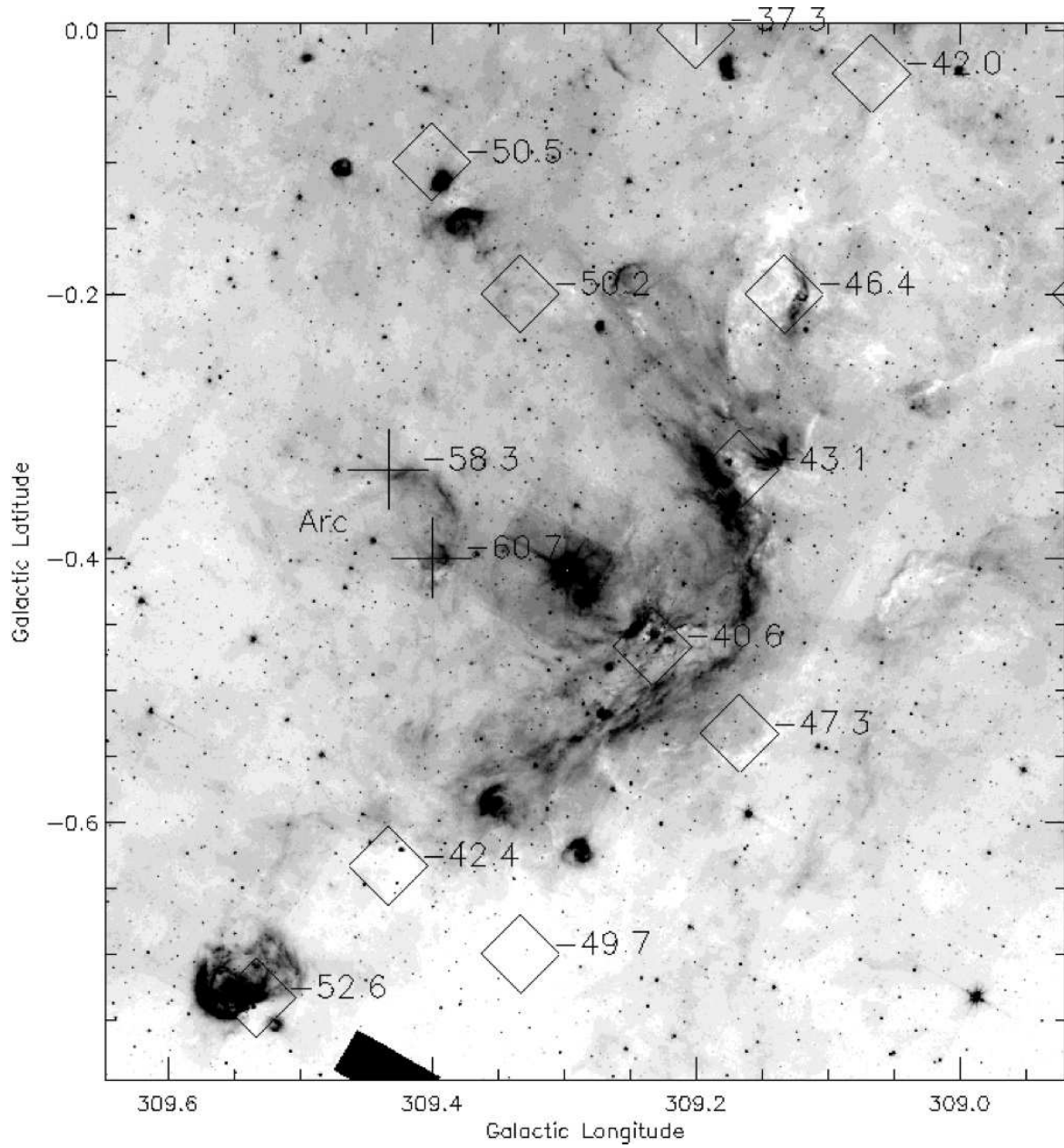


Fig. 3.— Gum 48d at 8 microns (left) tracing PAH emission. The positions of molecular clouds at velocities ranging from -36 to -64 km s^{-1} (the velocity of the Centaurus Arm) are marked, as listed in Saito et al. (2001). Diamonds indicate material in the velocity range of Gum 48d, crosses those clouds at slightly higher velocities. The infrared dark clouds can be seen as regions of no emission at 8 microns, here seen as light patches against the diffuse emission.

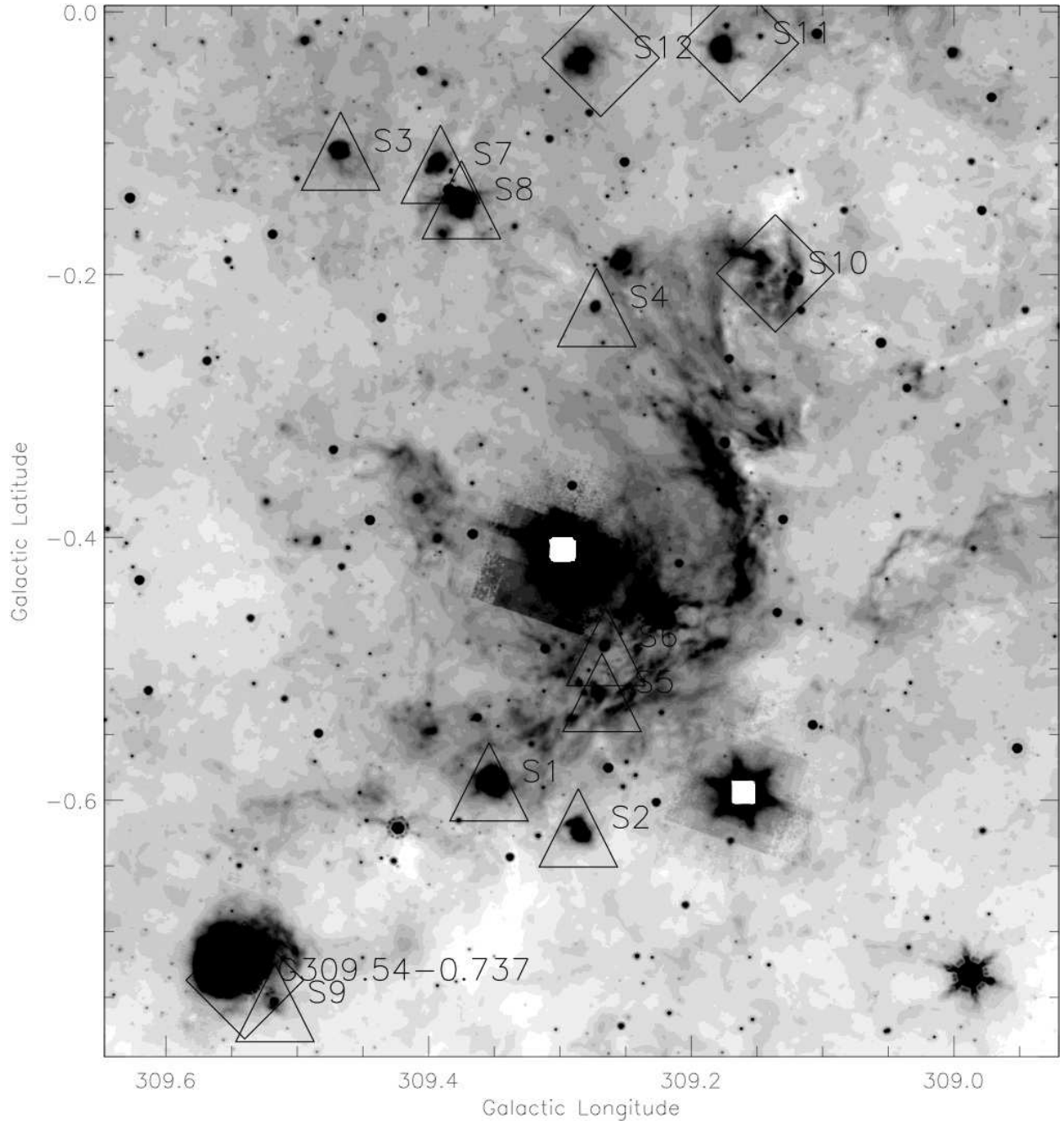


Fig. 4.— Gum 48d at 24 microns (left) tracing emission from warm dust. Diamonds mark the location of small HII region, while triangles mark the locations of the potential enshrouded B stars. The white squares are saturated pixels.

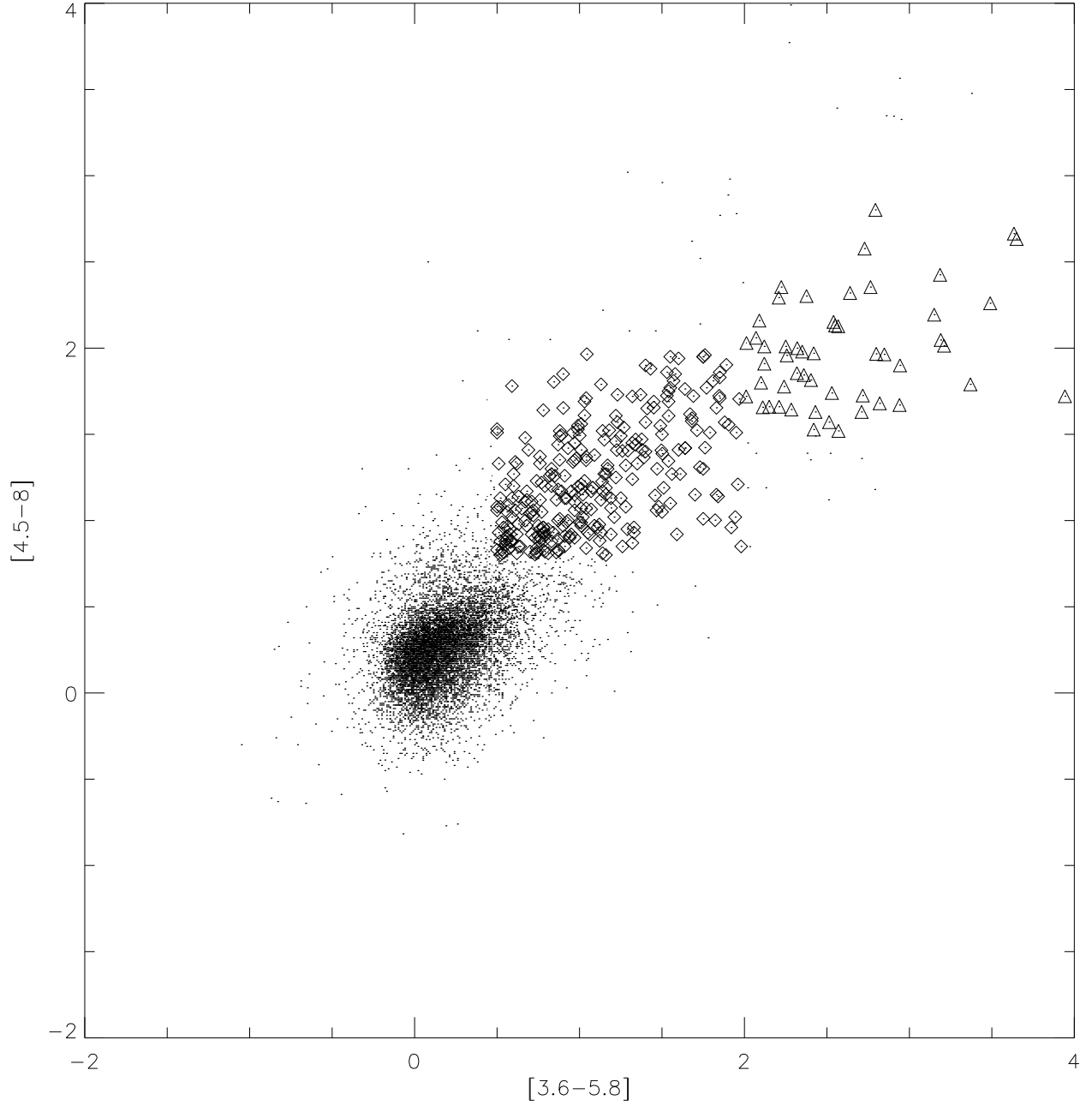


Fig. 5.— IRAC color-color diagram for Gum 48d. Triangles mark the Class I sources, diamonds the Class II and points the main sequence locus. Flat spectrum sources are not separated out in this technique.

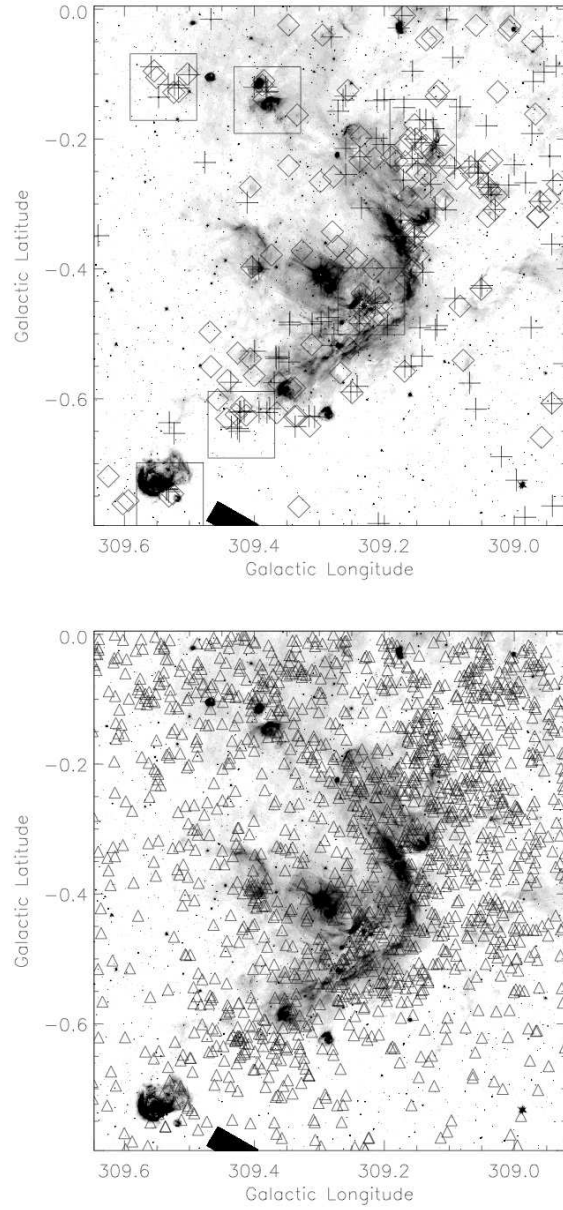


Fig. 6.— Gum 48d shown at 8 microns with star formation overlaid. Upper panel: Class I sources: crosses, Flat Spectrum: diamonds, with the location of clusters marked. Lower panel: class II sources marked with triangles.

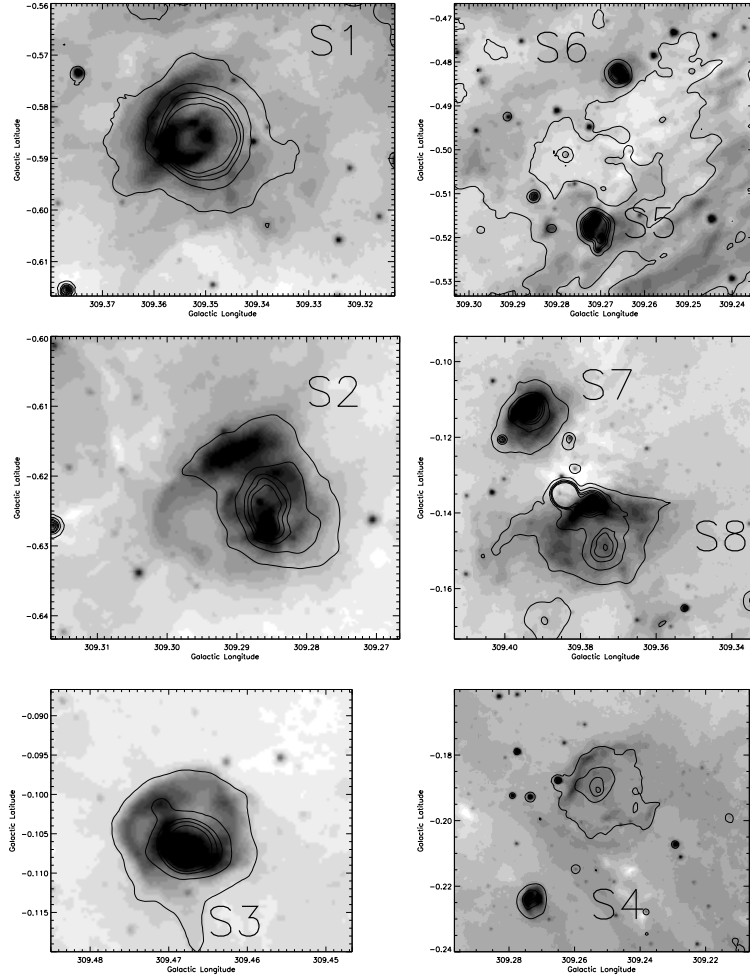


Fig. 7.— A gallery of compact features, shown at 8 microns (grey-scale) tracing PAH emission and 24 microns (contour) tracing warm dust. The source numbers are labeled.

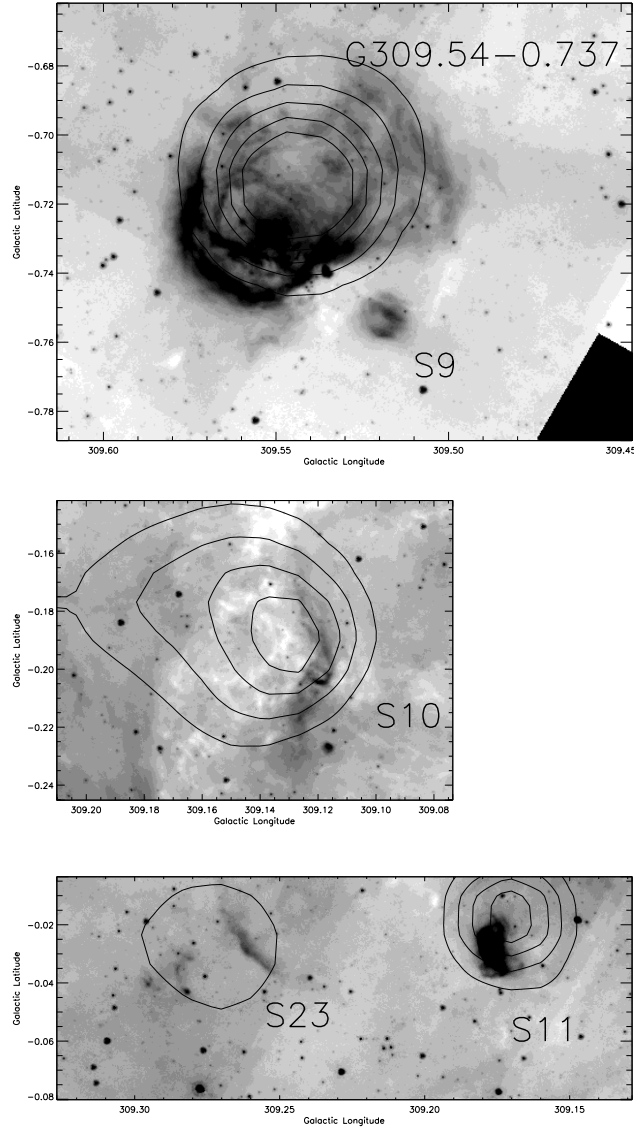


Fig. 8.— Compact features associated with emission from ionized gas. Greyscale: 8 micron PAH emission, Contour: 1420 MHz emission. The source numbers are labeled.

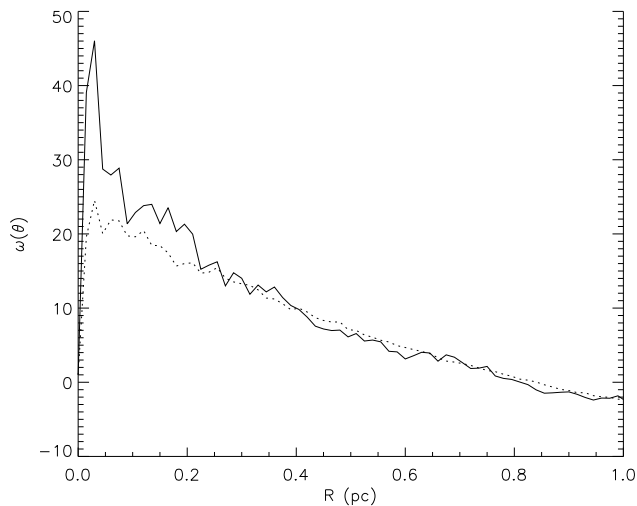


Fig. 9.— A schematic diagram of the history of Gum 48d. (a) ≈ 10 Myr ago: a giant HII region ionized by multiple OB stars creates a shell as it expands into giant molecular cloud, (b) ≈ 4 Myr ago: The giant HII region has consumed much of the cloud and has accelerated the surrounding molecular material. HR 5171A and B have formed at the periphery, in the surrounding shell, and have produced their own HII region, Gum 48d. (c) ≈ 1 Myr ago: The giant HII region is not longer present, as the ionizing stars have passed through the SN phase, and what is left is a low density region with a remnant expanding shell. Gum 48d is in its most energetic phase. (d) Present: The ionization balance of Gum 48d has changed considerably, as it is now ionized by a single B0 star. Between the HII region and the dense molecular cloud is a low density, un-ionized region, as the recombination timescale is short compared to the age of the region. This is the remnant of the more energetic HII region.

Table 1. Physical parameters of compact features in Gum 48d. The physical scale assumes a distance of 3.5 kpc.

| Source Number | glon | glat | IRAS ID | Diameter arcsec | Diameter pc | IRAS Flux $\log(L_{\odot})$ | Ionized Gas |
|---------------|---------|--------|-----------------|-----------------|-------------|-----------------------------|--------------|
| S1 | 309.354 | -0.586 | IRAS 13444-6230 | 69 | 1.3 | 3.52 | |
| S2 | 309.286 | -0.621 | IRAS 13439-6233 | 43 | 0.83 | 3.94 | |
| S3 | 309.467 | -0.106 | IRAS 13445-6200 | 33 | 0.64 | 3.46 | |
| S4 | 309.272 | -0.225 | | 15 | 0.29 | | |
| S5 | 309.268 | -0.518 | | 23 | 0.45 | | |
| S6 | 309.265 | -0.483 | | 32 | 0.62 | 3.77 | |
| S7 | 309.391 | -0.116 | IRAS 13439-6207 | 37 | 0.73 | 3.93 | |
| S8 | 309.375 | -0.143 | IRAS 13438-6203 | 77 | 1.5 | | |
| S9 | 309.517 | -0.754 | | 24 | 0.47 | | |
| S10 | 309.140 | -0.194 | IRAS 13418-6210 | 170 | 3.3 | | G309.14-0.18 |
| S11 | 309.176 | -0.030 | IRAS 13419-6159 | 68 | 1.3 | | G309.17-0.02 |
| S12 | 309.273 | -0.035 | | 99 | 1.9 | | G309.27-0.03 |

REFERENCES

- Adams, F. C., Shu, F. H., and Lada, C. J.: 1988, *ApJ* **326**, 865
- Allen, L. E., Calvet, N., D’Alessio, P., Merin, B., Hartmann, L., Megeath, S. T., Gutermuth, R. A., Muzerolle, J., Pipher, J. L., Myers, P. C., and Fazio, G. G.: 2004, *ApJS* **154**, 363
- Arthur, S. J.: 2007, in *Revista Mexicana de Astronomia y Astrofisica Conference Series*, Vol. 30 of *Revista Mexicana de Astronomia y Astrofisica Conference Series*, pp 64–71
- Benjamin, R. A., Churchwell, E., Babler, B. L., Bania, T. M., Clemens, D. P., Cohen, M., Dickey, J. M., Indebetouw, R., Jackson, J. M., Kobulnicky, H. A., Lazarian, A., Marston, A. P., Mathis, J. S., Meade, M. R., Seager, S., Stolovy, S. R., Watson, C., Whitney, B. A., Wolff, M. J., and Wolfire, M. G.: 2003, *PASP* **115**, 953
- Brand, J. and Blitz, L.: 1993, *A&A* **275**, 67
- Carey, S. J., Clark, F. O., Egan, M. P., Price, S. D., Shipman, R. F., and Kuchar, T. A.: 1998, *ApJ* **508**, 721
- Caswell, J. L. and Haynes, R. F.: 1987, *A&A* **171**, 261
- Caswell, J. L., Kesteven, M. J., Stewart, R. T., Milne, D. K., and Haynes, R. F.: 1992, *ApJ* **399**, L151
- Caswell, J. L., Milne, D. K., and Wellington, K. J.: 1981, *MNRAS* **195**, 89
- Caswell, J. L., Vaile, R. A., Ellingsen, S. P., Whiteoak, J. B., and Norris, R. P.: 1995, *MNRAS* **272**, 96
- Dewdney, P. E., Roger, R. S., Purton, C. R., and McCutcheon, W. H.: 1991, *ApJ* **370**, 243
- Diaz-Miller, R. I., Franco, J., and Shore, S. N.: 1998, *ApJ* **501**, 192
- Dyson, J. E. and Williams, D. A.: 1997, *The physics of the interstellar medium*, The physics of the interstellar medium. Edition: 2nd ed. Publisher: Bristol: Institute of Physics Publishing, 1997. Edited by J. E. Dyson and D. A. Williams. Series: The graduate series in astronomy. ISBN: 0750303069
- Elmegreen, B. G.: 1998, in C. E. Woodward, J. M. Shull, and H. A. Thronson, Jr. (eds.), *Origins*, Vol. 148 of *Astronomical Society of the Pacific Conference Series*, pp 150–+
- Elmegreen, B. G. and Lada, C. J.: 1977, *ApJ* **214**, 725

- Fuente, A., Martin-Pintado, J., Bachiller, R., Neri, R., and Palla, F.: 1998, *A&A* **334**, 253
- Fuente, A., Martin-Pintado, J., Bachiller, R., Rodriguez-Franco, A., and Palla, F.: 2002, *A&A* **387**, 977
- Garcia-Segura, G. and Franco, J.: 1996, *ApJ* **469**, 171
- Gaustad, J. E., McCullough, P. R., Rosing, W., and Van Buren, D.: 2001, *PASP* **113**, 1326
- Georgelin, Y. M., Boulesteix, J., Georgelin, Y. P., Le Coarer, E., and Marcelin, M.: 1988, *A&A* **205**, 95
- Green, D. A.: 2004, *Bulletin of the Astronomical Society of India* **32**, 335
- Gum, C. S.: 1955, *MmRAS* **67**, 155
- Guseinov, O. H., Ankey, A., and Tagieva, S. O.: 2004, *Serbian Astronomical Journal* **169**, 65
- Humphreys, R. M., Strecker, D. W., and Ney, E. P.: 1971, *ApJ* **167**, L35+
- Indebetouw, R., Mathis, J. S., Babler, B. L., Meade, M. R., Watson, C., Whitney, B. A., Wolff, M. J., Wolfire, M. G., Cohen, M., Bania, T. M., Benjamin, R. A., Clemens, D. P., Dickey, J. M., Jackson, J. M., Kobulnicky, H. A., Marston, A. P., Mercer, E. P., Stauffer, J. R., Stolovy, S. R., and Churchwell, E.: 2005, *ApJ* **619**, 931
- Karr, J. L., Manoj, P., and Ohashi, N.: 2008, *in preparation*
- Karr, J. L. and Martin, P. G.: 2003, *ApJ* **595**, 900
- Kerton, C. R.: 2002, *AJ* **124**, 3449
- Lefloch, B. and Lazareff, B.: 1994, *A&A* **289**, 559
- McClure-Griffiths, N. M., Dickey, J. M., Gaensler, B. M., Green, A. J., Haverkorn, M., and Strasser, S.: 2005, *ApJS* **158**, 178
- Perryman, M. A. C. and ESA (eds.): 1997, *The HIPPARCOS and TYCHO catalogues. Astrometric and photometric star catalogues derived from the ESA HIPPARCOS Space Astrometry Mission*, Vol. 1200 of *ESA Special Publication*
- Rakowski, C. E., Hughes, J. P., and Slane, P.: 2001, *ApJ* **548**, 258
- Robitaille, T. P., Whitney, B. A., Indebetouw, R., and Wood, K.: 2007, *ApJS* **169**, 328

- Rodgers, A. W., Campbell, C. T., and Whiteoak, J. B.: 1960, *MNRAS* **121**, 103
- Roger, R. S. and Dewdney, P. E.: 1992, *ApJ* **385**, 536
- Saito, H., Mizuno, N., Moriguchi, Y., Matsunaga, K., Onishi, T., Mizuno, A., and Fukui, Y.: 2001, *PASJ* **53**, 1037
- Schaerer, D. and de Koter, A.: 1997, *A&A* **322**, 598
- Schaller, G., Schaerer, D., Meynet, G., and Maeder, A.: 1992, *A&AS* **96**, 269
- Skrutskie, M. F., Cutri, R. M., Stiening, R., Weinberg, M. D., Schneider, S., Car embeddede-
diate masspenter, J. M., Beichman, C., Capps, R., Chester, T., Elias, J., Huchra, J.,
Liebert, J., Lonsdale, C., Monet, D. G., Price, S., Seitzer, P., Jarrett, T., Kirkpatrick,
J. D., Gizis, J. E., Howard, E., Evans, T., Fowler, J., Fullmer, L., Hurt, R., Light, R.,
Kopan, E. L., Marsh, K. A., McCallon, H. L., Tam, R., Van Dyk, S., and Wheelock,
S.: 2006, *AJ* **131**, 1163
- Tenorio-Tagle, G.: 1979, *A&A* **71**, 59
- Tenorio-Tagle, G. and Bodenheimer, P.: 1988, *ARA&A* **26**, 145
- Tielens, A. G. G. M. and Hollenbach, D.: 1985, *ApJ* **291**, 747
- Vacca, W. D., Garmany, C. D., and Shull, J. M.: 1996, *ApJ* **460**, 914
- van Genderen, A. M.: 1992, *A&A* **257**, 177
- Whiteoak, J. B. Z. and Green, A. J.: 1996, *A&AS* **118**, 329
- Whitworth, A. P., Bhattal, A. S., Chapman, S. J., Disney, M. J., and Turner, J. A.: 1994,
MNRAS **268**, 291